

Single-Edge and Double-Edge Cracks in a Fully Anisotropic Strip

Haiying Huang

Graduate Research Assistant.

George A. Kardomateas

Professor.

School of Aerospace Engineering,
Georgia Institute of Technology,
Atlanta, GA 30332-0150

The mode I and II stress intensity factors in a fully anisotropic infinite strip with a single-edge or double-edge crack configuration are obtained from an approach based on the continuous dislocation technique. The elastic solution of a single dislocation in an anisotropic half plane is used in conjunction with an array of dislocations along the boundary of the infinite strip, which is supposed to be traction-free, to provide the solution of a single dislocation in an anisotropic infinite strip. The dislocation densities of the dislocation array are determined in such a way that the traction forces generated by the dislocation array cancel the residual tractions along the boundary due to the single dislocation in the half plane. The stress field of a single dislocation in the infinite strip is thus a superposition of that of the single dislocation and the dislocation array in the half plane. This solution is then applied to calculate the mixed mode I and II stress intensity factors for a single-edge and a double-edge crack in the anisotropic strip, by replacing the cracks with a series of dislocations and satisfying the crack surface traction-free conditions. To illustrate the results, typical material data for graphite/epoxy were used in a unidirectional construction with the fiber orientation, θ , measured from the load direction (perpendicular to the crack direction), varying between 0 and 90 degrees. It is found that the effect of anisotropy on the mode I stress intensity factor is significant between 30 and 60 degrees and depends strongly on the relative crack length, being larger for cracks of relative larger length. The mode mixity, defined such that it is zero for pure mode I and 90 degrees for pure mode II, is significant between 40 and 70 degrees, and is in general between zero and 20 degrees.

Introduction

The extensive use of composites in the last decades for high performance, low weight structures motivates the need for modeling and predicting their structural behavior and failure modes. Especially, interlayer cracking (delamination) is a common failure mode of laminated composites. In most cases, these cracks are subjected to mixed-mode loading and the mode I and mode II stress intensity factors at the crack tip are needed in order to predict the propagation behavior. In addition to interlayer cracks, intra-layer cracking has been observed to take place in certain stacking sequences (Pelegri and Kardomateas, 1998).

Mixed-mode stress intensity factors can be calculated by various methods. A detailed review of stress intensity factor calculation can be found in Cartwright and Rooke (1975). One of the most effective methods is the distributed dislocation technique, which is a semi-analytical technique. The basic idea of the distributed dislocation technique is to model the cracks by continuous dislocations along the crack lines in otherwise perfect bodies. Hills et al. (1996) have a detailed description of applying the distributed dislocation technique to solve the isotropic crack problem. Based on an implementation of Bueckner's (1958) theorem, the crack problem is usually solved in three steps: first the traction forces along the cracks are found in the absence of the cracks. Second, the stresses due to dislocations along the crack lines are found in the same geometry. Finally, the distribution of dislocations is determined in such a way that the traction-free conditions along the crack surfaces are satisfied. In order to achieve this, an integral equation is established which typically must be solved by a nu-

merical method. The crack tip stress intensity factors can be normally calculated from the dislocation densities.

It should be stated that the continuous dislocation approach has been mostly applied in determining stress intensity factors for relatively simple configurations. This is because the number of fundamental solutions available for the various kind of dislocations is limited to simple geometries such as infinite space, half plane, near a circular inclusion, etc. In addition, the stress distribution of the structure without cracks should be easy to calculate. This is why many publications based on this method deal with infinite plates or strips subject to uniform far field loading (Gupta and Erdogan, 1974; Civelek and Erdogan, 1980; Civelek, 1985).

Very few papers have dealt with nonisotropic cracks in finite or semi-infinite bodies. An edge crack in a strip with edge loading was studied by Thouless et al. (1987) and by Suo (1990), whereas as far as solutions in orthotropic materials, the distributed dislocation method was employed by Suo (1990) and Suo and Hutchinson (1990) to obtain the stress intensity factors for an orthotropic strip. The method employed for the field in the unflawed strip was an Airy stress function solution with Fourier transforms. Suo (1990) also discussed the possible extension to an anisotropic strip. In earlier studies, Georgiadis and Papadopoulos (1987, 1988) investigated an orthotropic infinite strip with a semi-infinite crack mid-distance of the strip faces by using Fourier transforms in combination with the Wiener-Hopf technique. In a more recent study, Qian and Sun (1997) obtained stress intensity factors for interface cracks between two monoclinic media, by either calculating the finite-extension strain energy release rates or utilizing the relationships between the crack surface displacements and the stress intensity factors, both carried out with a finite element analysis.

A solution to the problem of a fully anisotropic strip with a single-edge or double-edge cracks is presented in this paper. A different approach than the Fourier transform method of Suo (1990) is followed in this paper. First, the elastic solution of a

Contributed by the Materials Division for publication in the JOURNAL OF ENGINEERING MATERIALS AND TECHNOLOGY. Manuscript received by the Materials Division February 2, 1999; revised manuscript received May 13, 1999. Guest Editors: Assimina A. Pelegri, Ann M. Sastry, and Robert Wetherhold.

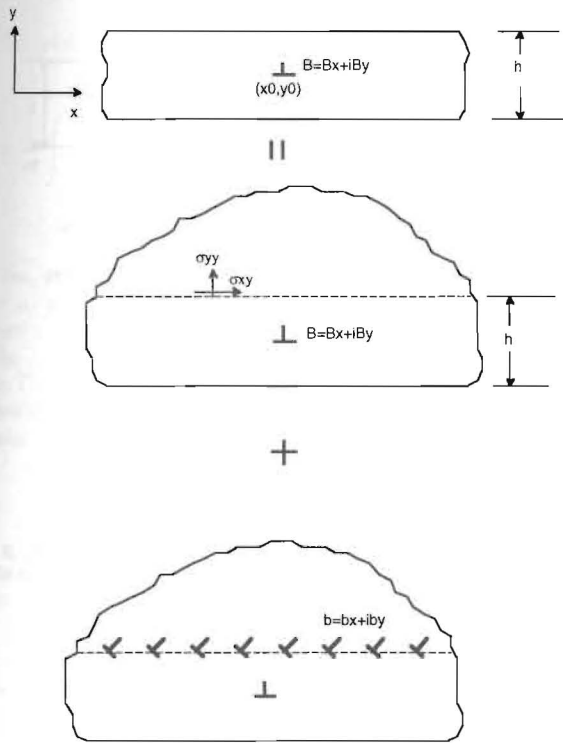


Fig. 1 Single dislocation in an infinite strip as a superposition of a single dislocation in a half plane and an array of dislocations at the boundary of the strip

dislocation in an anisotropic infinite strip is derived by assigning an array of dislocations along a line in the half plane which is supposed to be the boundary of the infinite strip. The dislocation densities of these added dislocations are determined by satisfying the traction-free boundary conditions. The stress fields of a single dislocation in the anisotropic strip is thus the combination of that of the single dislocation and those of the dislocations distributed along the boundary. Subsequently, the elastic solution is employed to calculate the mixed-mode stress intensity factors of single- and double-edge cracks in the anisotropic infinite strip. The material anisotropy and the crack length effects on the Mode I and II stress intensity factors are investigated.

Formulation

A Dislocation in a Fully Anisotropic Strip. As shown in Fig. 1, the geometry of a dislocation in an infinite strip can be decomposed into two geometries. The first one is a half plane with a single dislocation located at point (x_0, y_0) , for which the elastic solution of the dislocation can be found in Lee (1990) and is summarized in Appendix A. In short, the stress components at point (x, y) due to a dislocation $B = B_x + iB_y$ located at (x_0, y_0) can be expressed as:

$$\sigma_{ij}(x, y) = B_x(x_0, y_0)G_{xij}(x, y, x_0, y_0) + B_y(x_0, y_0)G_{yij}(x, y, x_0, y_0), \quad (1)$$

where $ij = xx, yy, xy$ and $G_{ij}(x, y, x_0, y_0)$ are the stress components at (x, y) due to a unit dislocation $B_x = 1$ at (x_0, y_0) and $G_{yij}(x, y, x_0, y_0)$ are the stress components at (x, y) due to a unit dislocation $B_y = 1$ at (x_0, y_0) .

Accordingly, the tractions along the dashed line, which is supposed to be the boundary of the infinite strip, due to the single dislocation $B(x_0, y_0)$ in the half plane are:

$$\sigma_{yy}^{(s)}(x, h) = B_x(x_0, y_0)G_{xyy}(x, h, x_0, y_0) + B_y(x_0, y_0)G_{yyy}(x, h, x_0, y_0), \quad (2a)$$

and,

$$\sigma_{xy}^{(s)}(x, h) = B_x(x_0, y_0)G_{xxy}(x, h, x_0, y_0) + B_y(x_0, y_0)G_{yyx}(x, h, x_0, y_0). \quad (2b)$$

The second geometry is a half plane with an array of dislocations along the dashed line. The dislocation densities of the dislocations $b(x, h)$ along the boundary are determined in such a way that the tractions generated by these dislocations along the dashed line $\sigma_{yy}^{(a)}(x, h)$ and $\sigma_{xy}^{(a)}(x, h)$ are the opposite of $\sigma_{yy}^{(s)}(x, h)$ and $\sigma_{xy}^{(s)}(x, h)$. Thus the traction-free boundary conditions of the infinite strip are satisfied after superposing these two geometries together. Suppose that the dislocation array $b(t, h) = b_x(t, h) + ib_y(t, h)$ are distributed from $-\infty$ to ∞ , then the tractions along the dashed line are:

$$\sigma_{yy}^{(a)}(x, h) = \int_{-\infty}^{\infty} [b_x(t, h)G_{xyy}(x, h, t, h) + b_y(t, h)G_{yyy}(x, h, t, h)]dt = -\sigma_{yy}^{(s)}(x, h), \quad (3a)$$

$$\sigma_{xy}^{(a)}(x, h) = \int_{-\infty}^{\infty} [b_x(t, h)G_{xxy}(x, h, t, h) + b_y(t, h)G_{yyx}(x, h, t, h)]dt = -\sigma_{xy}^{(s)}(x, h). \quad (3b)$$

where $\sigma_{ij}^{(s)}$ are defined in Eq. (2).

The functions $G_{xyy}(x, h, t, h)$, $G_{yyy}(x, h, t, h)$, $G_{xxy}(x, h, t, h)$ and $G_{yyx}(x, h, t, h)$ are singular at $x = t$. Since the single dislocation is in self-equilibrium, the tractions $\sigma_{yy}^{(s)}(x, h)$ and $\sigma_{xy}^{(s)}(x, h)$ vanish as $t \rightarrow -\infty, +\infty$. As a result, the dislocation densities $b_x(t, h)$ and $b_y(t, h)$ go to zero as $t \rightarrow -\infty, +\infty$. Therefore, for calculation purposes, in the singular integral equations (3) we can ignore the dislocations located at $x > d$ and $x < -d$, where d is a value large enough compared to h . A value of $d = 100h$ was found to be more than adequate for this purpose. Thus, Eqs. (3) become:

$$\sigma_{yy}^{(a)}(x, h) = \int_{-d}^d [b_x(t, h)G_{xyy}(x, h, t, h) + b_y(t, h)G_{yyy}(x, h, t, h)]dt = -\sigma_{yy}^{(s)}(x, h), \quad (4a)$$

$$\sigma_{xy}^{(a)}(x, h) = \int_{-d}^d [b_x(t, h)G_{xxy}(x, h, t, h) + b_y(t, h)G_{yyx}(x, h, t, h)]dt = -\sigma_{xy}^{(s)}(x, h). \quad (4b)$$

Now, normalize Eq. (4) as following:

$$\tilde{t} = \frac{t}{d} \quad \text{and} \quad \tilde{x} = \frac{x}{d}$$

so that these equations can be written in the form:

$$\sigma_{ij}^{(a)} = \pi d \left[\frac{1}{\pi} \int_{-1}^1 b_x(\tilde{t}, h)G_{xij}(x, h, t, h) + b_y(\tilde{t}, h)G_{yij}(x, h, t, h) \right]d\tilde{t} = -\sigma_{ij}^{(s)}(x, h), \quad ij = xx, xy \quad (5)$$

We can actually enforce that $b(\tilde{t}, h) = b_x(\tilde{t}, h) + ib_y(\tilde{t}, h)$ be zero at $\tilde{t} = -1$ and $\tilde{t} = 1$ ($t = -d$ and $t = d$) assuming that d is large enough. This can be built into the solution by expressing $b(\tilde{t}, h)$ as the product of a fundamental function $W(\tilde{t})$ and an unknown function $\tilde{b}(\tilde{t}, h)$ (Hills et al., 1996):

$$b(\bar{t}) = W(\bar{t})\bar{b}(\bar{t}, h); \quad W(\bar{t}) = \sqrt{1 - \bar{t}^2}. \quad (6)$$

Substituting Eq. (6) into Eq. (5), the numerical form of the singular integral equations can be expressed as:

$$\begin{aligned} \pi d \left[\sum_{i=1}^N W_i \bar{b}_x(\bar{t}_i, h) \bar{G}_{xij}(x_k, h, t_i, h) \right. \\ \left. + \sum_{i=1}^N W_i \bar{b}_y(\bar{t}_i, h) \bar{G}_{yij}(x_k, h, t_i, h) \right] = -\sigma_{ij}^{(d)}(x_k, h), \end{aligned} \quad (7)$$

$ij = xx, xy \quad k = 1, \dots, N+1$

where \bar{t}_i are the N discrete integral points and \bar{x}_k are the collocation points and W_i are the weight coefficients:

$$\begin{aligned} \bar{t}_i = \cos \left(\frac{\pi i}{N+1} \right); \quad \bar{x}_k = \cos \left[\frac{\pi(2k-1)}{2(N+1)} \right]; \\ W_i = \frac{1 - \bar{t}_i^2}{N+1}. \end{aligned} \quad (8)$$

Equation (7) allows us to determine the dislocation densities $b(\bar{t}_i, h)$ of the dislocation array along the dashed line, which cancel out the residual tractions due to a single dislocation $B(x_0, y_0)$ in the first geometry. After the dislocation densities $b(\bar{t}_i, h)$ are known, the stress components at every point (x, y) in the second geometry can be calculated as following,

$$\begin{aligned} \sigma_{ij}^{(d)}(x, y) = \pi d \left[\sum_{i=1}^N W_i \bar{b}_x(\bar{t}_i, h) \bar{G}_{xij}(x, y, t_i, h) \right. \\ \left. + \sum_{i=1}^N W_i \bar{b}_y(\bar{t}_i, h) \bar{G}_{yij}(x, y, t_i, h) \right], \end{aligned} \quad (9)$$

where $ij = xx, yy$ and xy .

Obviously, the dislocation densities $b(\bar{t}_i, h)$ along the dashed line are related to the single dislocation $B(x_0, y_0)$ in the half plane. Denoting the dislocation densities $b(\bar{t}_i, h)$ as $b^{(x)}(\bar{t}_i, h) = b_x^{(x)}(\bar{t}_i, h) + ib_y^{(x)}(\bar{t}_i, h)$ for a single dislocation $B(x_0, y_0) = 1$ and as $b^{(y)}(\bar{t}_i, h) = b_x^{(y)}(\bar{t}_i, h) + ib_y^{(y)}(\bar{t}_i, h)$ for a dislocation $B(x_0, y_0) = i$, and superposing these two elastic fields, we have:

$$\begin{aligned} \bar{G}_{xij}(x, y) = G_{xij}(x, y) + \pi d \left[\sum_{i=1}^N W_i \bar{b}_x^{(x)}(\bar{t}_i, h) G_{xij}(x, y, t_i, h) \right. \\ \left. + \sum_{i=1}^N W_i \bar{b}_y^{(x)}(\bar{t}_i, h) G_{yij}(x, y, t_i, h) \right], \end{aligned} \quad (10a)$$

and

$$\begin{aligned} \bar{G}_{yij}(x, y) = G_{yij}(x, y) + \pi d \left[\sum_{i=1}^N W_i \bar{b}_x^{(y)}(\bar{t}_i, h) G_{xij}(x, y, t_i, h) \right. \\ \left. + \sum_{i=1}^N W_i \bar{b}_y^{(y)}(\bar{t}_i, h) G_{yij}(x, y, t_i, h) \right], \end{aligned} \quad (10b)$$

where $ij = xx, yy$ and xy .

Physically, $\bar{G}_{xij}(x, y)$ in Eq. (10a) represent the stresses at (x, y) due to a dislocation $B_x = 1$ at (x_0, y_0) in the infinite strip; Similarly, $\bar{G}_{yij}(x, y)$ in Eq. (10b) represent the stresses at (x, y) due to a dislocation $B_y = 1$ at (x_0, y_0) in the infinite strip. Because of the linearity of the elastic fields of the dislocation, the stress

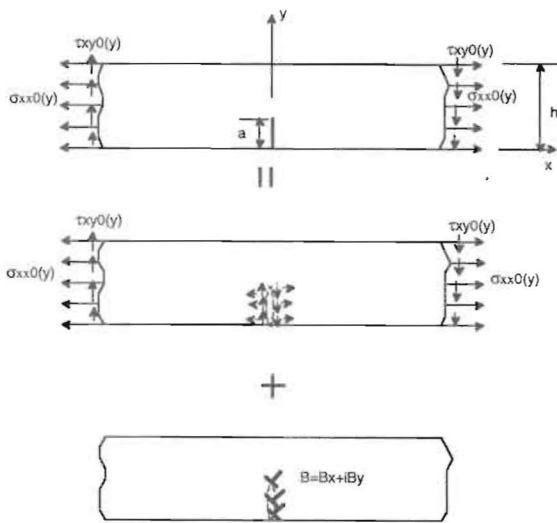


Fig. 2 Single-edge crack represented by an array of dislocations, $B = B_x + iB_y$, determined so that the traction-free conditions at the crack site are satisfied

components at (x, y) due to a dislocation $B(x_0, y_0) = B_x(x_0, y_0) + iB_y(x_0, y_0)$ in the infinite strip are:

$$\begin{aligned} \sigma_{ij}(x, y) = B_x(x_0, y_0) \bar{G}_{xij}(x, y, x_0, y_0) \\ + B_y(x_0, y_0) \bar{G}_{yij}(x, y, x_0, y_0), \end{aligned} \quad (11)$$

Next, this elastic solution of the dislocation in an anisotropic infinite strip is used in the single-edge crack and the double-edge crack configuration.

A Single Edge Crack Under Uniform Tension. An infinite strip with an edge crack subjected to uniform tension is considered next. As shown in Fig. 2, the edge crack, of length a , is located in the lower half of the infinite strip and is aligned with the y axis. Thus, the crack tip is at $y = a$. Replacing the crack with a series of dislocations, we find that the singular integral equations that ensure crack surface traction-free condition for the edge crack are:

$$\begin{aligned} \sigma_{xx}^{(d)}(0, y) = \int_0^a [B_x(0, t) \bar{G}_{xxx}(0, y, 0, t) \\ + B_y(0, t) \bar{G}_{yxx}(0, y, 0, t)] dt = -\sigma_0, \end{aligned} \quad (12a)$$

and

$$\begin{aligned} \sigma_{xy}^{(d)}(0, y) = \int_0^a [B_x(0, t) \bar{G}_{xxy}(0, y, 0, t) \\ + B_y(0, t) \bar{G}_{yyx}(0, y, 0, t)] dt = 0. \end{aligned} \quad (12b)$$

The foregoing equations ensure that the tractions $\sigma_{xx}^{(d)}$ and $\sigma_{xy}^{(d)}$ cancel out the tractions along the crack face due to the external loading, which is σ_0 in our case. It should be mentioned that the edge crack is a surface-breaking crack and the stress components are not singular at both ends of the crack. The Gaussian quadrature, which would be employed to solve the singular integral equations, has to be chosen carefully so that it includes all the appropriate end-point asymptotics. First, the integral equations are normalized through the following substitutions:

$$\bar{t} = \frac{2t - a}{a}, \quad \bar{y} = \frac{2y - a}{a}$$

so that Eqs. (12) can be written in the following form:

$$\sigma_{ij}^{(d)}(0, y) = \pi a \left[\frac{1}{\pi} \int_{-1}^1 B_x(0, \bar{t}) \bar{G}_{xij}(0, y, 0, t) d\bar{t} + \frac{1}{\pi} \int_{-1}^1 B_y(0, \bar{t}) \bar{G}_{yij}(0, y, 0, t) d\bar{t} \right] = -\sigma_{ij}^{(s)}(y) \quad ij = xx, xy \quad (13)$$

Now, $B_x(\bar{t})$ and $B_y(\bar{t})$ must be singular at the crack tips $\bar{t} = 1$ ($t = a$) and bounded at $\bar{t} = -1$ ($t = 0$). Note that it has been proven by Stroh (1958) that the crack tip stresses have a singularity of the $r^{-1/2}$ type in anisotropic materials, just as in the isotropic case. Thus, the dislocation density $B(\bar{t})$ should be expressed in the following product of a fundamental function $W(\bar{t})$ and an unknown regular function $\bar{B}(\bar{t})$:

$$B(\bar{t}) = W(\bar{t})\bar{B}(\bar{t}); \quad W(\bar{t}) = \sqrt{\frac{1+\bar{t}}{1-\bar{t}}} \quad (14)$$

Substituting Eq. (14) into Eq. (13), the numerical form of the singular integral equations can be expressed as:

$$\pi a \left\{ \sum_{i=1}^N W_i \bar{B}_x(0, \bar{t}_i) \bar{G}_{xxx}(0, y_k, 0, t_i) + \sum_{i=1}^N W_i \bar{B}_y(0, \bar{t}_i) \bar{G}_{yxx}(0, y_k, 0, t_i) \right\} = -\sigma_0 \quad k = 1 \dots N \quad (15a)$$

where \bar{t}_i are the N discrete integration points and \bar{y}_k are the N collocation points and W_i are weight coefficients:

$$\bar{t}_i = \cos \left(\pi \frac{2i-1}{2N+1} \right); \quad \bar{y}_k = \cos \left(\pi \frac{2k}{2N+1} \right); \quad W_i = \frac{2(1+\bar{t}_i)}{2N+1}$$

Also, $y_k = (a\bar{y}_k + a)/2$ and $t_i = (a\bar{t}_i + a)/2$. Similarly:

$$\pi a \left\{ \sum_{i=1}^N W_i \bar{B}_x(0, \bar{t}_i) \bar{G}_{xyy}(0, y_k, 0, t_i) + \sum_{i=1}^N W_i \bar{B}_y(0, \bar{t}_i) \bar{G}_{yyx}(0, y_k, 0, t_i) \right\} = 0, \quad k = 1 \dots N \quad (15b)$$

As there are $2N$ collocation points and $2N$ integral points, Eqs. (15) are sufficient for the determination of the dislocation density $\bar{B}(0, \bar{t}_i) = \bar{B}_x(0, \bar{t}_i) + i\bar{B}_y(0, \bar{t}_i)$ along the edge crack. Of major significance is the value of the dislocation density at the crack tip, $\bar{B}(+1)$, as it is directly related to the stress intensity factors. It can be obtained from Krenk's interpolation formulae (Hills et al., 1996):

$$\bar{B}(+1) = M_E \sum_{i=1}^N B_E \bar{B}(\bar{t}_i), \quad (16)$$

where

$$M_E = \frac{2}{2N+1}, \quad \text{and}$$

$$B_E = \cot \left(\frac{2i-1}{2N+1} \frac{\pi}{2} \right) \sin \left(\frac{2i-1}{2N+1} N\pi \right)$$

The stress intensity factor at the crack tip $y = a$, is defined as:

$$K_I + iK_{II} = \lim_{y \rightarrow a} \left\{ \sqrt{2\pi(a-y)} [\sigma_{xx}(y) + i\tau_{xy}(y)] \right\}_{y=0} \quad (17a)$$

Using relations for the stresses in terms of the complex potentials as in (A3), gives

$$K_I + iK_{II} = \lim_{y \rightarrow a} \left\{ \sqrt{2\pi(a-y)} \sum_{j=1,2} (\mu_j^2 - i\mu_j) \phi_j'(z_j) + (\bar{\mu}_j^2 - i\bar{\mu}_j) \bar{\phi}_j'(z_j) \right\} \quad (17b)$$

Only the singular part of the stress potential contributes, which is due to a dislocation at the crack tip, i.e., as $y \rightarrow a$ and $z \rightarrow z_0$, therefore the first term becomes (see also Appendix):

$$\phi_1'(z_1) = \frac{A_1}{z_1 - z_{10}} \rightarrow \frac{A_{11}b(y)dy + A_{12}\bar{b}(y)dy}{dz_1} = \frac{A_{11}b(y)dy + A_{12}\bar{b}(y)dy}{\mu_1 dy} \quad (17c)$$

Therefore, the first term in (17b) gives

$$\lim_{y \rightarrow a} \sqrt{2\pi(a-y)} (\mu_1 - i) [A_{11}b(y) + A_{12}\bar{b}(y)], \quad (17d)$$

and with the substitution $\bar{t} = (2y - a)/a$ and $b(y) = \bar{B}(\bar{t})\sqrt{(1-\bar{t})/(1+\bar{t})}$, it gives

$$\lim_{t \rightarrow 1} \sqrt{\pi a(1-\bar{t})} (\mu_1 - i) [A_{11}\bar{B}(\bar{t}) + A_{12}\bar{\bar{B}}(\bar{t})] \sqrt{\frac{1+\bar{t}}{1-\bar{t}}} = \sqrt{2\pi a} (\mu_1 - i) [A_{11}\bar{B}(+1) + A_{12}\bar{\bar{B}}(+1)] \quad (17e)$$

A similar contribution exists from the μ_2 term.

And the stress intensity factors at the crack tip $y = a$ are related to the dislocation densities at the crack tip as follows:

$$K_I + iK_{II} = \sqrt{2\pi a} \left\{ [(\mu_1 - i)A_{11} + (\mu_2 - i)A_{21} + (\bar{\mu}_1 - i)\bar{A}_{12} + (\bar{\mu}_2 - i)\bar{A}_{22}] \bar{B}(+1) + [(\mu_1 - i)A_{12} + (\mu_2 - i)A_{22} + (\bar{\mu}_1 - i)\bar{A}_{11} + (\bar{\mu}_2 - i)\bar{A}_{21}] \bar{\bar{B}}(+1) \right\}, \quad (18)$$

where $A_{11}, A_{12}, A_{21}, A_{22}$ are defined in Appendix A and $\bar{B}(+1)$ is given in (16). Notice that $\bar{\bar{B}}(+1)$ is the complex conjugate of $\bar{B}(+1)$.

Double Edge Cracks Under Uniform Tension. Another geometry we studied is a rectangular plate with double edge cracks subjected to uniform external load. Two edge cracks are of length a and located symmetrically about the middle plane of the infinite strip. Both cracks are aligned with the y axis. The lower edge crack is denoted as crack I and the upper edge crack as crack II.

The crack surface traction-free conditions in Eq. (12) is for a single edge crack and can be easily extended to the case of double edge cracks. Choosing coordinate systems for edge crack I and II as $y^{(i)}$ and $t^{(i)}$ ($i = 1, 2$), the expressions for the crack surface tractions yield the following systems of singular integral equations:

$$\sigma_{ij}^{(d)}(y^{(m)}) = \int_0^a B_x(0, t^{(1)}) \bar{G}_{xij}(0, y^{(m)}, 0, t^{(1)}) dt^{(1)} + \int_0^a B_y(0, t^{(1)}) \bar{G}_{yij}(0, y^{(m)}, 0, t^{(1)}) dt^{(1)}$$

$$\begin{aligned}
& + \int_{h-a}^h b_x(0, t^{(2)}) \tilde{G}_{xij}(0, y^{(m)}, 0, t^{(2)}) dt^{(2)} \\
& + \int_{h-a}^h b_y(0, t^{(2)}) \tilde{G}_{yij}(0, y^{(m)}, 0, t^{(2)}) dt^{(2)} = -\sigma_{ij}^{(\sigma)}(y^{(m)}), \\
& ij = xx, xy \quad \text{and} \quad m = 1, 2, \quad (19)
\end{aligned}$$

Again, the integral equations are normalized through the following substitutions:

$$\bar{y}^{(1)} = \frac{2y^{(1)}}{a} - 1, \quad \bar{t}^{(1)} = \frac{2t^{(1)}}{a} - 1,$$

and

$$\bar{y}^{(2)} = \frac{2y^{(2)}}{a} - \left(\frac{2h}{a} - 1\right), \quad \bar{t}^{(2)} = \frac{2t^{(2)}}{a} - \left(\frac{2h}{a} - 1\right),$$

so that Eqs. (19) can be written in the form:

$$\begin{aligned}
\pi a \sum_{j=1}^2 \left[\frac{1}{\pi} \int_{-1}^1 B_x(\bar{t}^{(j)}) \tilde{G}_{xij}(y^{(m)}, t^{(j)}) d\bar{t}^{(j)} \right. \\
\left. + \frac{1}{\pi} \int_{-1}^1 B_y(\bar{t}^{(j)}) \tilde{G}_{yij}(y^{(m)}, t^{(j)}) d\bar{t}^{(j)} \right] = -\sigma_{ii}^{(\sigma)}(y^{(m)}) \quad ii \\
= xx, xy \quad \text{and} \quad m = 1, 2. \quad (20)
\end{aligned}$$

$B_x(\bar{t}^{(1)})$ and $B_y(\bar{t}^{(1)})$ must be singular at the crack tip $\bar{t}^{(1)} = 1$ ($t^{(1)} = a$) and bounded at the edge $\bar{t}^{(1)} = -1$ ($t^{(1)} = 0$). The form of $B_x(\bar{t}^{(2)})$ and $B_y(\bar{t}^{(2)})$ are the opposite of that of $B_x(\bar{t}^{(1)})$ and $B_y(\bar{t}^{(1)})$, i.e., $B_x(\bar{t}^{(2)})$ and $B_y(\bar{t}^{(2)})$ are bounded at $\bar{t}^{(2)} = 1$ ($t^{(2)} = h$) and singular at $\bar{t}^{(2)} = -1$ ($t^{(2)} = h - a$). Expressing $B(\bar{t}^{(1)})$ and $B(\bar{t}^{(2)})$ as

$$B(\bar{t}^{(1)}) = W^{(1)}(\bar{t}^{(1)}) \bar{B}(\bar{t}^{(1)}); \quad W^{(1)}(\bar{t}^{(1)}) = \sqrt{\frac{1 + \bar{t}^{(1)}}{1 - \bar{t}^{(1)}}} \quad (21a)$$

$$B(\bar{t}^{(2)}) = W^{(2)}(\bar{t}^{(2)}) \bar{B}(\bar{t}^{(2)}); \quad W^{(2)}(\bar{t}^{(2)}) = \sqrt{\frac{1 - \bar{t}^{(2)}}{1 + \bar{t}^{(2)}}} \quad (21b)$$

and substituting Eq. (21) into Eq. (20), the numerical form of the singular integral equations can be expressed as:

$$\begin{aligned}
\pi a \sum_{j=1}^2 \left\{ \sum_{i=1}^N W_i^{(j)} \bar{B}_x(\bar{t}_i^{(j)}) \tilde{G}_{xij}(y_k^{(m)}, t_i^{(j)}) \right. \\
\left. + \sum_{i=1}^N W_i^{(j)} \bar{B}_y(\bar{t}_i^{(j)}) \tilde{G}_{yij}(y_k^{(m)}, t_i^{(j)}) \right\} = -\sigma_{ij}^{(\sigma)}(y_k^{(m)}) \\
k = 1 \dots N, \quad m = 1, 2 \quad \text{and} \quad ij = xx, xy \quad (22)
\end{aligned}$$

where $\bar{t}_i^{(j)}$ are the $2N$ discrete integration points; $\bar{y}_k^{(m)}$ are the $2N$ collocation points and $W_i^{(j)}$ are weight coefficients:

$$\bar{t}_i^{(1)} = \cos \left[\frac{\pi(2i-1)}{2N+1} \right]; \quad \bar{y}_k^{(1)} = \cos \left[\frac{\pi 2k}{2N+1} \right];$$

$$W_i^{(1)} = \frac{2(1 + \bar{t}_i^{(1)})}{2N+1}$$

and

$$\bar{t}_i^{(2)} = \cos \left[\pi \frac{2i}{2N+1} \right]; \quad \bar{y}_k^{(2)} = \cos \left[\pi \frac{2k-1}{2N+1} \right];$$

$$W_i^{(2)} = \frac{2(1 - \bar{t}_i^{(2)})}{2N+1}$$

Also, $y_k^{(1)} = (a\bar{y}_k^{(1)} + a)/2$, $t_i^{(1)} = (a\bar{t}_i^{(1)} + a)/2$ and $y_k^{(2)} = (a/2)\bar{y}_k^{(2)} + (h - (a/2))$, $t_i^{(2)} = (a/2)\bar{t}_i^{(2)} + (h - (a/2))$.

Now we have $4N$ linear equations to solve for the $4N$ unknowns, i.e., $\bar{B}^{(1)}(\bar{t}_i^{(1)}) = \bar{B}_x(\bar{t}_i^{(1)}) + i\bar{B}_y(\bar{t}_i^{(1)})$ and $\bar{B}^{(2)}(\bar{t}_i^{(2)}) = \bar{B}_x(\bar{t}_i^{(2)}) + i\bar{B}_y(\bar{t}_i^{(2)})$ can be solved at the discrete set of points $\bar{t}_i^{(1)}$ and $\bar{t}_i^{(2)}$ from Eqs. (22).

Again, the value of $\bar{B}^{(1)}(+1)$ and $\bar{B}^{(2)}(-1)$ can be obtained from Krenk's interpolation formulas (Hills et al., 1996):

$$B_z^{(1)}(+1) = M_z^{(1)} \sum_{i=1}^N B_z^{(1)}(\bar{t}_i^{(1)}), \quad (23a)$$

$$B_z^{(2)}(-1) = M_z^{(2)} \sum_{i=1}^N B_z^{(2)}(\bar{t}_{N+1-i}^{(2)}), \quad (23b)$$

where

$$M_z^{(1)} = \frac{2}{2N+1}, \quad B_z^{(1)} = \cot \left[\frac{2i-1}{2N+1} \frac{\pi}{2} \right] \sin \left[\frac{2i-1}{2N+1} N\pi \right]$$

and

$$M_z^{(2)} = 1, \quad B_z^{(2)} = \sin \left[\frac{i\pi}{2N+1} (2N-1) \right] \csc \left[\frac{i\pi}{2N+1} \right]$$

In a similar fashion to the single edge crack, the stress intensity factors at $y = a$ can be related to the dislocation densities from the following expression:

$$\begin{aligned}
(K_I + iK_{II})|_a = \sqrt{2\pi a} \{ [(\mu_1 - i)A_{11} + (\mu_2 - i)A_{21} \\
+ (\bar{\mu}_1 - i)\bar{A}_{12} + (\bar{\mu}_2 - i)\bar{A}_{22}] B_z^{(1)}(+1) + [(\mu_1 - i)A_{12} \\
+ (\mu_2 - i)A_{22} + (\bar{\mu}_1 - i)\bar{A}_{11} + (\bar{\mu}_2 - i)\bar{A}_{21}] \bar{B}_z^{(1)}(+1) \}. \quad (24)
\end{aligned}$$

Similarly, the stress intensity factors at the other crack tip, $y = h - a$, are:

$$\begin{aligned}
(K_I + iK_{II})|_{h-a} = -\sqrt{2\pi a} \{ [(\mu_1 - i)A_{11} + (\mu_2 - i)A_{21} \\
+ (\bar{\mu}_1 - i)\bar{A}_{12} + (\bar{\mu}_2 - i)\bar{A}_{22}] B_z^{(2)}(-1) + [(\mu_1 - i)A_{12} \\
+ (\mu_2 - i)A_{22} + (\bar{\mu}_1 - i)\bar{A}_{11} + (\bar{\mu}_2 - i)\bar{A}_{21}] \bar{B}_z^{(2)}(-1) \}. \quad (25)
\end{aligned}$$

Discussion of Results

For an isotropic single edge crack under uniform tension, the mode I stress intensity factor expression given by Tada et al. (1985) is:

$$K_I = F\sigma\sqrt{\pi a};$$

$$F = 0.265(1 - \alpha)^4 + \frac{0.857 + 0.265\alpha}{(1 - \alpha)^{3/2}}, \quad (26)$$

where $\alpha = a/h$. The comparison of present results (discrete points) and those from Tada's formula (continuous line) are shown in Fig. 3(a). The agreement is satisfactory with the relative error within 9%. It should be mentioned that the isotropic solutions were calculated from the present fully anisotropic formulation by setting the complex parameters $\mu_1 = 1.0001i$ and $\mu_2 = 0.9999i$.

The effects of material anisotropy on the mode I stress intensity factors and the mode mixity for a single edge crack under uniform tension are shown in Figs. 3(b) and 3(c). Typical data for graphite/epoxy were used, i.e., moduli in GPa: $E_L = 130$, $E_T = 10.5$, $G_{LT} = 6$ and Poisson's ratio $\nu_{LT} = 0.28$, where L and T are the directions along and perpendicular to the fibers, respectively. A

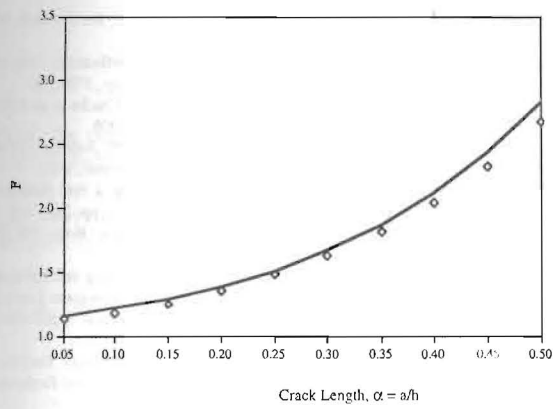


Fig. 3(a) Mode I stress intensity factor parameter, F , in $K_I = F\sigma\sqrt{\pi a}$, for an isotropic, single-edge crack in a strip under uniform tension, σ . The line is the Tada et al. (1985) relationship for an isotropic crack and the discrete data points are from the present anisotropic formulation when taken at the limit of isotropy.

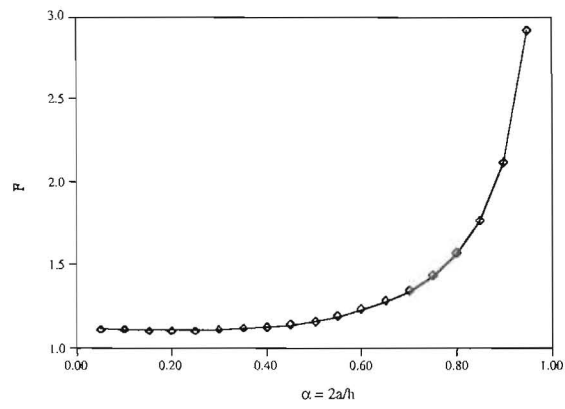


Fig. 4(a) Mode I stress intensity factor parameter, F , in $K_I = F\sigma\sqrt{\pi a}$, for an isotropic, double-edge crack in a strip under uniform tension, σ . The line is the Tada et al. (1985) relationship for an isotropic crack and the discrete data points are from the present anisotropic formulation when taken at the limit of isotropy.

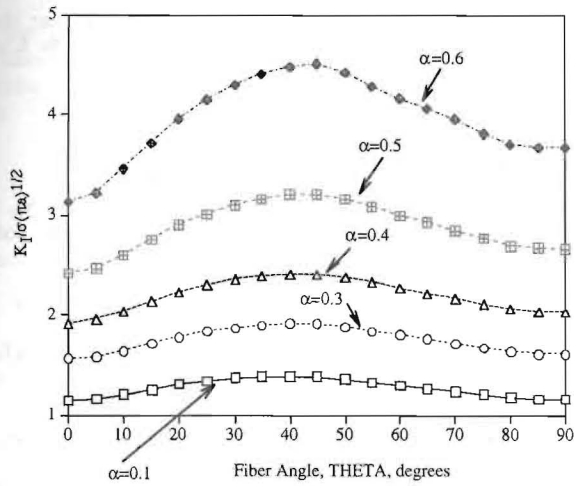


Fig. 3(b) The effect of anisotropy on the mode I stress intensity factor of a single-edge crack in a strip under uniform tension for a unidirectional graphite/epoxy with fiber orientation, θ , measured from the direction of the applied load. The stress intensity factor, K_I , is normalized with the corresponding stress intensity factor of an isotropic, infinite plate, $\sigma\sqrt{\pi a}$.

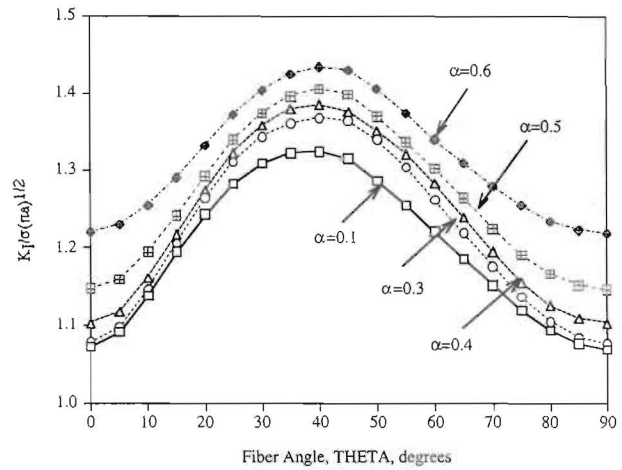


Fig. 4(b) The effect of anisotropy on the mode I stress intensity factor of a double-edge crack configuration in a strip under uniform tension for a unidirectional graphite/epoxy with fiber orientation, θ , measured from the direction of the applied load. The length of each of the two cracks is a and the applied uniform tension is σ .

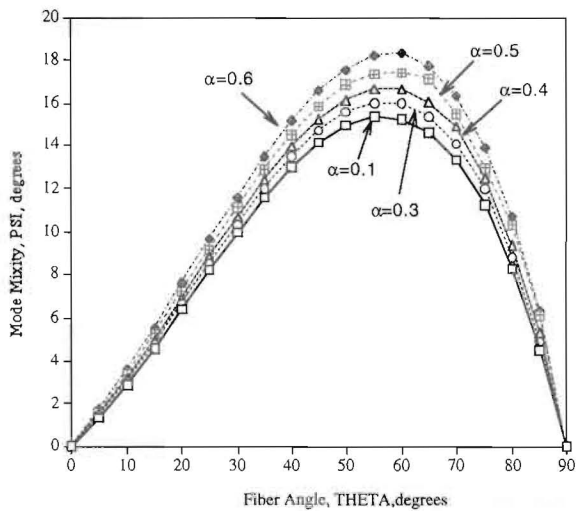


Fig. 3(c) The effect of anisotropy on the mode mixity, ψ , of a single-edge crack in a strip under uniform tension for a unidirectional graphite/epoxy with fiber orientation, θ , measured from the direction of the applied load. The zero degrees correspond to pure mode I. A pure mode II case would give 90 degrees.

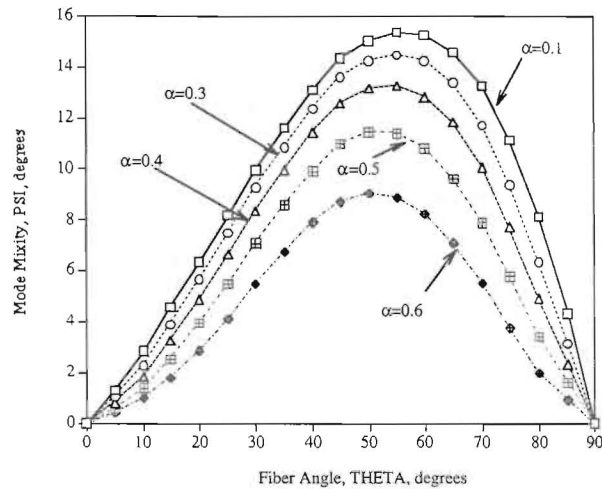


Fig. 4(c) The effect of anisotropy on the mode mixity, ψ , of a double-edge crack configuration in a strip under uniform tension for a unidirectional graphite/epoxy with fiber orientation, θ , measured from the direction of the applied load. The zero and 90 degree fiber angles are the orthotropic limits, corresponding to pure mode I, $\psi = 0$.

unidirectional construction was considered with the fiber orientation angle, θ , varying from 0 to 90 degrees. The orientation angle θ is measured from the x direction, i.e., $\theta = 0$ deg is when the crack is perpendicular to the fibers and $\theta = 90$ deg is when the crack is parallel to the fibers. Obviously, the limits of $\theta = 0$ and 90 deg are the orthotropic cases. Both the normalized mode I stress intensity factors and the mode mixities increase as the relative length $\alpha = a/h$ increases. Because the crack is not symmetric, the mode I stress intensity factors at fiber orientation 0 and 90 deg are different and the difference is more obvious for longer cracks. In addition, the anisotropic single edge crack is under mixed-mode loading even though the external load is uniform and the crack is relatively short. As shown in Fig. 3(b) the effect of anisotropy on the mode I stress intensity factors is seen to be significant between 30 and 60 degrees and depends also on the relative crack length $\bar{a} = a/h$, being larger for cracks of relative larger length. The mode mixity ψ in Fig. 3(c) is defined as

$$\psi = \tan^{-1} \left(\frac{K_{II}}{K_I} \right),$$

and expresses the relative amounts of mode I and mode II components. As expected, the mode II stress intensity factors are zero for orthotropic materials. The effect of anisotropy on the mode mixity is dependent on both the fiber orientation and the relative crack length. The fiber angle at which the mode mixity is maximum shifts to the higher angles as the relative crack length increases.

The other example we investigated is a rectangular plate with double edge cracks. The mode I stress intensity factors for an isotropic rectangular plate with double edge cracks under uniform tension are given by Tada et al. (1985):

$$K_I = F\sigma\sqrt{\pi a};$$

$$F = \left(1 + 0.122 \cos^4 \frac{\pi\alpha}{2} \right) \sqrt{\frac{2}{\pi\alpha} \tan \left(\frac{\pi\alpha}{2} \right)}, \quad (27)$$

where $\alpha = 2a/h$. Figure 4(a) compares the values of F calculated from the present method (discrete points) and those obtained from Eq. (27) (continuous line), which indicates a very good agreement. The effect of anisotropy on both the mode I stress intensity factor and the mode mixity for double edge cracks under uniform tension is shown in Fig. 4(b) and Fig. 4(c). The effect of anisotropy on the mode I stress intensity factor is seen to be noteworthy at fiber angles 30 to 60 degrees, as in the single edge crack case. On the other hand, the mode mixity decreases as the edge cracks become longer and the crack tips are far away from the boundaries. Such differences in the behavior between a single and double-edge crack configuration are not surprising due to the lack of symmetry in the single-edge crack case, as opposed to the symmetric double-edge crack.

Acknowledgments

The financial support of the Office of Naval Research, Ship Structures S& T Division, Grant N00014-91-J-1892, and of the Army Research Office through CERT, Grant NCC2-945, and the interest and encouragement of the Grant Monitors Dr. Y. D. S. Rajapakse and Dr. G. Anderson, are both gratefully acknowledged.

References

- Bueckner, H. F., 1958, "The Propagation of Cracks and the Energy of Elastic Deformation," *ASME Journal of Applied Mechanics*, Vol. 80, pp. 1225-1230.
- Cartwright, D. J., and Rooke, D. P., 1975, "Evaluation of Stress Intensity Factors," *J. of Strain Analysis*, Vol. 10, No. 4, pp. 217-262.
- Civelek, M. B., and Erdogan, F., 1982, "Crack Problems for a Rectangular Plate and an Infinite Strip," *Int. J. of Fract.*, Vol. 19, pp. 139-159.
- Civelek, M. B., 1985, "Stress Intensity Factors for a System of Cracks in an Infinite Strip," *Fracture Mechanics*, Sixteenth Symposium, ASTM, Philadelphia, pp. 7-26.
- Georgiadis, H. G., and Papadopoulos, G. A., 1987, "Determination of SIF in a

Cracked Plane Orthotropic Strip by the Wiener-Hopf Technique," *Int. J. Fract.*, Vol. 34, pp. 57-64.

Georgiadis, H. G., and Papadopoulos, G. A., 1988, "Cracked Orthotropic Strip with Clamped Boundaries," *J. Appl. Math. Phys. (ZAMP)*, Vol. 39, pp. 573-578.

Gupta, G. D., and Erdogan, F., 1974, "The Problem of Edge Cracks in an Infinite Strip," *ASME Journal of Applied Mechanics*, Dec., pp. 1001-1006.

Hills, D. A., Kelly, P. A., Di, D. N., and Korsunsky, A. M., 1996, *Solution of Crack Problems; the Distributed Dislocation Technique*, Kluwer Academic, U.K.

Lee, J. C., 1990, "Analysis of a Fiber Bridged Crack Near a Free Surface in Ceramic Matrix Composites," *Eng. Fract. Mech.*, Vol. 37, No. 1, pp. 209-219.

Lekhnitskii, S. G., 1981, *Theory of Elasticity of an Anisotropic Body*, Mir Publishers, Moscow.

Pelegri, A. A., and Kardomateas, G. A., 1998, "Intralayer Cracking in Delaminated Glass/Epoxy and Graphite/Epoxy Laminates Under Cyclic or Monotonic Loading," *Proceedings, 39th AIAA/ASME/ASCE/AHS/ASC SDM Conference*, April 20-23, Long Beach, CA, pp. 1534-1544, Paper no. AIAA-98-1879.

Qian, W., and Sun, C. T., 1997, "Calculation of Stress Intensity Factors for Interlaminar Cracks in Composite Laminates," *Composite Science and Technology*, Vol. 57, pp. 637-650.

Stroh, A. N., 1958, "Dislocations and Cracks in Anisotropic Elasticity," *Philosophical Magazine*, Vol. 3, pp. 625-646.

Suo, Z., and Hutchinson, J. W., 1990, "Interface Crack between Two Elastic Layers," *Inter. J. of Fracture*, Vol. 43, pp. 1-18.

Suo, Z., 1990, "Delamination Specimens for Orthotropic Materials," *ASME Journal of Applied Mechanics*, Vol. 57, Sep., pp. 627-634.

Tada, H., Paris, P. C., and Irwin, G. R., 1985, *The Stress Analysis of Cracks Handbook*, 2nd Edition, Paris Productions, St. Louis.

Thouless, M. D., Evans, A. G., Ashby, M. F., and Hutchinson, J. W., 1987, "The Edge Cracking and Spalling of Brittle Plates," *Acta Meta.*, Vol. 35, No. 6, pp. 1333-1341.

APPENDIX

A Dislocation in an Anisotropic Half Plane

Let us consider a state of plane strain, i.e., $\epsilon_{zz} = \gamma_{yz} = \gamma_{xz} = 0$. In this case, the stress-strain relations for the anisotropic body are (Lekhnitskii, 1981):

$$\begin{bmatrix} \epsilon_{xx} \\ \epsilon_{yy} \\ \epsilon_{zz} \\ \gamma_{xy} \end{bmatrix} = \begin{bmatrix} \alpha_{11} & \alpha_{12} & \alpha_{13} & \alpha_{16} \\ \alpha_{12} & \alpha_{22} & \alpha_{23} & \alpha_{26} \\ \alpha_{13} & \alpha_{23} & \alpha_{33} & \alpha_{36} \\ \alpha_{16} & \alpha_{26} & \alpha_{36} & \alpha_{66} \end{bmatrix} \begin{bmatrix} \sigma_{xx} \\ \sigma_{yy} \\ \sigma_{zz} \\ \tau_{xy} \end{bmatrix}, \quad (A1a)$$

where α_{ij} are the compliance constants (we have used the notation $1 \equiv x, 2 \equiv y, 3 \equiv z, 6 \equiv xy$).

Using the condition of plane strain, which requires that $\epsilon_{zz} = 0$, allows elimination of σ_{zz} , i.e.,

$$\sigma_{zz} = -\frac{1}{\alpha_{33}} (\alpha_{13}\sigma_{xx} + \alpha_{23}\sigma_{yy}). \quad (A1b)$$

Equations (1a) can then be written in the form

$$\begin{bmatrix} \epsilon_{xx} \\ \epsilon_{yy} \\ \gamma_{xy} \end{bmatrix} = \begin{bmatrix} \beta_{11} & \beta_{12} & \beta_{16} \\ \beta_{12} & \beta_{22} & \beta_{26} \\ \beta_{16} & \beta_{26} & \beta_{66} \end{bmatrix} \begin{bmatrix} \sigma_{xx} \\ \sigma_{yy} \\ \tau_{xy} \end{bmatrix}, \quad (A1c)$$

where

$$\beta_{ij} = \alpha_{ij} - \frac{\alpha_{i3}\alpha_{j3}}{\alpha_{33}} \quad (i, j = 1, 2, 6). \quad (A1d)$$

Problems of this type can be formulated in terms of two complex analytic functions $\phi_k(z_k)$ ($k = 1, 2$) of the complex variables $z_k = x + \mu_k y$, where $\mu_k, \bar{\mu}_k, k = 1, 2$ are the roots of the algebraic equation:

$$\beta_{11}\mu^4 - 2\beta_{16}\mu^3 + (\beta_{12} + \beta_{66})\mu^2 - 2\beta_{26}\mu + \beta_{22} = 0. \quad (A2)$$

It was proven by Lekhnitskii (1981) that these roots $\mu_1, \mu_2, \bar{\mu}_1, \bar{\mu}_2$ are either complex or purely imaginary, i.e., Eq. (2) cannot have real roots. Here, μ_1 and μ_2 are chosen to be the ones with positive imaginary parts.

The stress and displacement components can be expressed in terms of $\Phi_k(z_k)$ as (Lekhnitskii, 1981):

$$\sigma_{xx} = 2 \operatorname{Re}[\mu_1^2 \phi_1'(z_1) + \mu_2^2 \phi_2'(z_2)], \quad (A3a)$$

$$\sigma_{yy} = 2 \operatorname{Re}[\phi_1'(z_1) + \phi_2'(z_2)], \quad (\text{A3b})$$

$$\tau_{xy} = -2 \operatorname{Re}[\mu_1 \phi_1'(z_1) + \mu_2 \phi_2'(z_2)], \quad (\text{A3c})$$

Now, the complex stress potentials at a point $z = x + iy$ due to a single dislocation at $z_0 = x_0 + iy_0$ in an anisotropic half plane are given by Lee (1990). Only the results are presented here.

The derivatives of the complex stress potentials at z due to a dislocation at z_0 , are given as:

$$\phi_1'(z_1, z_0) = \frac{A_1}{z_1 - z_{10}} + \frac{1}{\Delta} \left[(\bar{\gamma}_1 \gamma_2 - \bar{\delta}_1 \delta_2) \frac{\bar{A}_1}{z_1 - \bar{z}_{10}} + (\gamma_2 \bar{\gamma}_2 - \delta_2 \bar{\delta}_2) \frac{\bar{A}_2}{z_1 - \bar{z}_{20}} \right], \quad (\text{A4a})$$

$$\phi_2'(z_2, z_0) = \frac{A_2}{z_2 - z_{20}} - \frac{1}{\Delta} \left[(\gamma_1 \bar{\gamma}_1 - \delta_1 \bar{\delta}_1) \frac{\bar{A}_1}{z_2 - \bar{z}_{10}} + (\gamma_1 \bar{\gamma}_2 - \delta_1 \bar{\delta}_2) \frac{\bar{A}_2}{z_2 - \bar{z}_{20}} \right]. \quad (\text{A4b})$$

The first terms in $\phi_1'(z_1, z_0)$, $\phi_2'(z_2, z_0)$ are the singular solutions for an infinite domain and the second terms are the regular solutions pertinent to a half plane. The material coefficients are:

$$\gamma_k = 1 - i\mu_k; \quad \delta_k = 1 + i\mu_k,$$

$$k = 1, 2 \quad \text{and} \quad \Delta = \gamma_1 \delta_2 - \gamma_2 \delta_1. \quad (\text{A4c})$$

Also,

$$z_i = [(1 - i\mu_i)z + (1 + i\mu_i)\bar{z}]/2, \quad i = 1, 2 \quad (\text{A4d})$$

The complex coefficients A_1 and A_2 are related to dislocation densities $b = b_x + ib_y$ as:

$$A_1 = A_{11}b + A_{12}\bar{b} \quad (\text{A5a})$$

$$A_2 = A_{21}b + A_{22}\bar{b} \quad (\text{A5b})$$

Then, $\bar{\phi}_1^{(s)'}(z_1)$, $\bar{\phi}_2^{(s)'}(z_2)$ and $\bar{\phi}_1^{(v)'}(z_1)$, $\bar{\phi}_2^{(v)'}(z_2)$ can be calculated from Eqs. (A4), (A5) by setting $b = 1$ and $b = i$, respectively. Subsequently, the stresses G_{xij} and G_{yij} can be determined from the complex stress potentials. For example,

$$G_{xxx} = 2 \operatorname{Re}[\mu_1^2 \bar{\phi}_1^{(s)'} + \mu_2^2 \bar{\phi}_2^{(s)'}].$$

The complex parameters A_{ij} are material properties, which can be found as follows. A_j constitute the solution of the following equations:

$$\begin{bmatrix} \delta_1 & -\bar{\gamma}_1 & \delta_2 & -\bar{\gamma}_2 \\ -\gamma_1 & \bar{\delta}_1 & -\gamma_2 & \bar{\delta}_2 \\ p(\mu_1) & -\bar{p}(\bar{\mu}_1) & p(\mu_2) & -\bar{p}(\bar{\mu}_2) \\ -\bar{p}(\mu_1) & p(\bar{\mu}_1) & -\bar{p}(\mu_2) & p(\bar{\mu}_2) \end{bmatrix} \begin{Bmatrix} A_1 \\ \bar{A}_1 \\ A_2 \\ \bar{A}_2 \end{Bmatrix} = \begin{Bmatrix} 0 \\ 0 \\ b/2\pi i \\ -\bar{b}/2\pi i \end{Bmatrix}, \quad (\text{A6a})$$

where

$$p(\mu_k) = (\beta_{12} - \beta_{16}\mu_k + \beta_{11}\mu_k^2) + i(\beta_{22} - \beta_{26}\mu_k + \beta_{12}\mu_k^2)/\mu_k$$

$$\text{and} \quad \bar{p}(\mu_k) = \overline{p(\bar{\mu}_k)}. \quad (\text{A6b})$$

Therefore, if we denote by A_r the solution to (A6) for $b = 1$ and by A_i the solution to (A6) for $b = i$, then from (A5), for $b = 1$,

$$A_1 = A_{11} + A_{12} = A_r(1); \quad A_2 = A_{21} + A_{22} = A_r(3)$$

and for $b = i$,

$$A_1 = A_{11}i - A_{12}i = A_i(1); \quad A_2 = A_{21}i - A_{22}i = A_i(3)$$

and these four equations can be solved for A_{ij} , $i, j = 1, 2$. For example,

$$A_{11} = [A_r(1) - iA_i(1)]/2. \quad (\text{A7})$$